Scleral hypoxia is a target for myopia control

Hao Wu[a,b,c,d,1], Wei Chen[e,1], Fei Zhao[a,b,c,d,1], Qingyi Zhou[a,b,c,d], Peter S. Reinach[a,b,c,d], Lili Deng[e,f], Li Ma[a,b,c,d], Shumeng Luo[e,f], Nethrajeith Srinivasalu[a,b,c,d], Miaozhen Pan[a,b,c,d], Yang Hu[a,b,c,d], Xiaomeng Pei[a,b,c,d], Jing Sun[a,b,c,d], Ran Ren[a,b,c,d], Yinghui Xiong[a,b,c,d], Zhonglou Zhou[a,b,c,d], Sen Zhang[a,b,c,d], Geng Tian[g], Jianhuo Fang[g], Lina Zhang[g], Jidong Lang[g], Deng Wu[e,f], Changqing Zeng[e,f,2], Jia Qu[a,b,c,d,2], and Xiangtian Zhou[a,b,c,d,2]

[a]School of Optometry and Ophthalmology Wenzhou Medical University, Wenzhou, 325027 Zhejiang, China; [b]Eye Hospital, Wenzhou Medical University, Wenzhou, 325027 Zhejiang, China; [c]State Key Laboratory of Optometry, Ophthalmology, and Vision Science, Wenzhou, 325027 Zhejiang, China; [d]Zhejiang Provincial Key Laboratory of Ophthalmology and Optometry, Wenzhou, 325027 Zhejiang, China; [e]Key Laboratory of Genomic and Precision Medicine, Beijing Institute of Genomics, The Chinese Academy of Sciences, 100101 Beijing, China; [f]University of Chinese Academy of Sciences, 100049 Beijing, China; and [g]Genomic and Synthetic Biology Core Facility, Tsinghua University, 100084 Beijing, China

Edited by Alexander Gentle, Deakin University, and accepted by Editorial Board Member Jeremy Nathans June 20, 2018 (received for review December 9, 2017)

Worldwide, myopia is the leading cause of visual impairment. It results from inappropriate extension of the ocular axis and concomitant declines in scleral strength and thickness caused by extracellular matrix (ECM) remodeling. However, the identities of the initiators and signaling pathways that induce scleral ECM remodeling in myopia are unknown. Here, we used single-cell RNA-sequencing to identify pathways activated in the sclera during myopia development. We found that the hypoxia-signaling, the eIF2-signaling, and mTOR-signaling pathways were activated in murine myopic sclera. Consistent with the role of hypoxic pathways in mouse model of myopia, nearly one third of human myopia risk genes from the genome-wide association study and linkage analyses interact with genes in the hypoxia-inducible factor-1α (HIF-1α)–signaling pathway. Furthermore, experimental myopia selectively induced HIF-1α up-regulation in the myopic sclera of both mice and guinea pigs. Additionally, hypoxia exposure (5% O_2) promoted myofibroblast transdifferentiation with down-regulation of type I collagen in human scleral fibroblasts. Importantly, the antihypoxia drugs salidroside and formononetin down-regulated HIF-1α expression as well as the phosphorylation levels of eIF2α and mTOR, slowing experimental myopia progression without affecting normal ocular growth in guinea pigs. Furthermore, eIF2α phosphorylation inhibition suppressed experimental myopia, whereas mTOR phosphorylation induced myopia in normal mice. Collectively, these findings defined an essential role of hypoxia in scleral ECM remodeling and myopia development, suggesting a therapeutic approach to control myopia by ameliorating hypoxia.

scleral hypoxia | myopia | scRNA-seq | HIF-1α | scleral ECM remodeling

Myopia, also known as "short-sightedness," is the leading cause of visual impairment in the world (1). It is emerging as a major public health concern (2) as we have witnessed a nearly pandemic increase in prevalence over the last two decades. In 2000, 1.406 billion people were myopic (22.9% of the world population) with 163 million (2.7% of the world population) presenting with high myopia of −6.00 diopters or worse. The worldwide prevalence is predicted to increase to 49.8% by 2050, with 9.8% being highly myopic (3). The most common corrective measure is to prescribe spectacle lenses, which correct the mismatch between ocular axial length and ocular refractive power, thus restoring normal vision. However, myopia is of particular concern because it is the dominant risk factor of blinding ocular diseases such as myopic maculopathy, retinal detachment, glaucoma, and cataract. For each of these conditions, the risk increases along with the increased degree of myopia (4). While interventions for myopia control such as spending more time outdoors, orthokeratology, and application of topical atropine frequently can prevent the onset or decelerate the progression of myopia (5), their effectiveness is limited as their mechanisms of action and the underlying pathogenesis of myopia are still elusive. Thus, there is an urgent need to better define the underlying pathogenesis and to develop effective and safe therapeutic interventions for prevention of myopia-related complications and vision loss.

In 1977, Wiesel and Raviola (6) reported the first animal model of myopia, and the exploration of alternative models and methods to investigate the mechanisms by which myopia develops has since expanded rapidly (7, 8). Myopia development is associated with excessive ocular axial elongation, thus causing the retina to lie behind the focal plane of the eye. In animal models of myopia (9, 10) and in humans (11), this change is accompanied by thinning of the sclera, the structural framework that maintains ocular shape and integrity. The scleral changes in different myopic models have prompted studies to delineate the mechanisms underlying scleral thinning and weakening during myopia development. These studies have shown that myopia-related remodeling of the scleral extracellular matrix (ECM) is linked to the decelerated synthesis and accelerated degradation of ECM components (12). This weakens the scleral framework

Significance

Myopia is the leading cause of visual impairment. Myopic eyes are characterized by scleral extracellular matrix (ECM) remodeling, but the initiators and signaling pathways underlying scleral ECM remodeling in myopia are unknown. In the present study, we found that hypoxia-inducible factor-1α (HIF-1α) signaling promoted myopia through myofibroblast transdifferentiation. Furthermore, antihypoxic treatments prevented the HIF-1α–associated molecular changes, thus suppressing myopia progression. Our findings defined the importance of hypoxia in scleral ECM remodeling and myopia development. The identification of the scleral hypoxia in myopia not only provides a concept for understanding the mechanisms of myopia development but also suggests viable therapeutic approach to control myopia progression in humans.

Author contributions: C.Z., J.Q., and X.Z. designed research; H.W., W.C., F.Z., Q.Z., L.M., S.L., M.P., Y.H., X.P., J.S., R.R., Y.X., Z.Z., S.Z., J.F., and L.Z. performed research; H.W., W.C., L.D., S.L., G.T., J.L., and D.W. analyzed data; H.W., W.C., F.Z., P.S.R., N.S., C.Z., J.Q., and X.Z. wrote the paper; and F.Z., J.Q., and X.Z. acquired funding.

The authors declare no conflict of interest.

This article is a PNAS Direct Submission. A.G. is a guest editor invited by the Editorial Board.

Data deposition: The primary sequencing datasets generated during the current study are available in the BioProject of the Genome Sequence Archive, bigd.big.ac.cn/bioproject/ (accession no. PRJCA000717).

[1]H.W., W.C., and F.Z. contributed equally to this work.

[2]To whom correspondence may be addressed. Email: czeng@big.ac.cn, jqu@wmu.edu.cn, or zxt@mail.eye.ac.cn.

This article contains supporting information online at www.pnas.org/lookup/suppl/doi:10.1073/pnas.1721443115/-/DCSupplemental.

Published online July 9, 2018.

and thereby enables increases in ocular elongation. For example, type I collagen is the major scleral ECM component, and declines in its expression weaken the scleral structural framework. During myopia development, type I collagen turnover increases due to down-regulation of its synthesis along with increased degradation (13, 14). Despite such insights and numerous experimental models that have been developed, the physiological signals that trigger these changes remain elusive. Critical questions remain regarding how myopia-associated scleral ECM remodeling is induced. One speculation is that visual signals in the retina produce unknown molecules that initiate responses in the choroid. In turn, the choroid generates signals that pass to the sclera and induce ECM remodeling and regulate the rate of ocular growth (12). While genetic or pharmacological studies have implicated the involvement of several molecular signals, including retinoic acid (15, 16), acetylcholine (17, 18), retinal dopamine (19), scleral TGF-β receptor-mediated signaling (20), and adenosine A2A receptors (21, 22) in myopia development, the nature of the mediators communicating from the retina to sclera remains unknown.

Molecular dissection of the mechanisms underlying scleral remodeling has been hampered by the lack of a method to address cellular heterogeneity within the scleral tissues. The mammalian sclera is composed of a single fibrous layer of connective tissue containing a heterogeneous cell population that includes sparsely distributed fibroblasts and myofibroblasts within an expansive collagenous ECM (23). Fibroblasts secrete type I collagen, which is the major component of collagen fibers, and other ECM components. Myofibroblasts are contractile cells that arise from stepwise transdifferentiation of fibroblasts and are identified by specific biomarkers such as vimentin, S100a4, periostin, and α-smooth muscle actin (α-SMA) (24). In addition, immune-induced infiltrating macrophages and dendritic cells are also present (25). However, it has been experimentally difficult to isolate each of these different scleral cell types and analyze them for identifying cell-specific signaling candidates that trigger scleral ECM remodeling and myopia development. So far, studies have used whole scleral tissue to characterize how changes in ocular length, accompanied by scleral alterations, lead to the thinning and extension of this structural framework. This global approach has limited ability to detect the local and cell-specific signaling molecular changes within the sclera that contribute to myopia development.

Single-cell RNA-sequencing (scRNA-seq) has been applied to resolve the complexity of different cell types in the retina (26). In this study, we used scRNA-seq to uncover scleral cell populations with distinct gene-expression profiles that account for the cellular phenotypic changes (i.e., fibroblasts-to-myofibroblast transdifferentiation) and the ECM alterations in sclera during myopia pathogenesis. Importantly, the results of this high-throughput technique enabled us to discover a mechanism, scleral hypoxia, which initiates a signaling cascade that leads to scleral ECM remodeling accounting for myopia development. We further established the causal role of scleral hypoxia during myopia development and the potential therapeutic ability of two anti-hypoxia drugs to control and limit myopia progression. Our results support the hypothesis that ameliorating scleral hypoxia is a viable therapeutic approach to improve control of myopia progression in humans.

Results

scRNA-Seq Reveals a Phenotypic Shift from Fibroblast to Myofibroblasts Following Form Deprivation. Using the Fluidigm C1 System, we determined the transcriptomes of 93 single cells isolated from form-deprivation (FD) scleras; untreated fellow eyes served as control. Forty-nine of the cells were from four scleral samples (each sample contained six to eight scleral tissues) of FD eyes; 44 cells originated from three samples (from similarly pooled scleras) of control eyes (*SI Appendix*, Table S1). The content of each single-cell library is listed in *SI Appendix*, Table S2. To select single scleral cells with high similarity to one another, three publicly available mouse scRNA-seq datasets (Gene Expression Omnibus accession nos. GSE60781, GSE47835, and GSE45719) (*SI Appendix*, Table S3) were included as controls in a cell–cell correlation analysis of their gene-expression patterns (*SI Appendix*, Fig. S1*A*). These cells formed four clusters in which single cells had similar profiles of correlation coefficients. As positive controls, most of the dendritic cells (GSE60781) formed cluster III, and two murine fibroblast cell lines (GSE47835 and GSE45719) formed cluster IV. Notably, the expression pattern of 71 cells from our data (cluster I) were strongly correlated with each other. In contrast, the remaining 22 cells were poorly correlated with each other, forming a cluster (cluster II) with two negative controls of mouse embryo fibroblasts (MEF-7 and MEF-8 from the GSE47835 dataset) (*SI Appendix*, Fig. S1*A*). These data indicate that the scRNA expression profiles of the 22 cells were similar to random amplification without cells. Furthermore, the fraction of cells with a poor mapping rate (<40%) was significantly higher in these 22 cells than in the remaining 71 cells ($P = 0.034$, χ^2 test); hence the subset of 22 cells was excluded from further analysis. The remaining cells expressed cellular markers characteristic of a fibroblast-like phenotype based on high expression levels of *Vim*, *Col1a1*, and *Col1a2* (Fig. 1*A* and *SI Appendix*, Fig. S1*B*). Some of them also highly expressed *S100a4*, *Acta2*, *Postn*, *Fap*, and *Ddr2*, which are ubiquitously expressed at different stages of myofibroblast transdifferentiation (24). *Ptprc* and *Des*, the markers for leukocytes and myocytes, respectively, were expressed at extremely low levels in the single cells (Fig. 1*A* and *SI Appendix*, Fig. S1*B*), suggesting that leukocytes and myocytes should be excluded from this population.

By calculating the squared coefficient of variation (CV^2) of the expression level for each gene among 71 scleral fibroblasts, we identified 4,463 genes displaying more heterogeneity in expression than could arise by chance (Fig. 1*B*). After unsupervised hierarchical clustering of these genes, the remaining 71 cells were divided into two major populations, designated as A1 and A2, containing 20 and 51 cells, respectively (Fig. 1*C*). We excluded cell cycle as a factor contributing to the subgrouping (*SI Appendix*, Fig. S2). There was no experimental bias in the subgrouping, as shown by the lack of any difference in the number of mapped reads in the A1 and A2 populations (*SI Appendix*, Fig. S3*A*).

Although both the A1 and A2 fibroblast populations existed in both FD and control eyes, the proportion of A2 cells was significantly higher in the FD eyes than in the control eyes (Fig. 1*D*). This difference in population composition suggested that there was a phenotypic shift in the distribution and abundance of myofibroblast subtypes within the FD eyes during myopia development. Both the number of expressed genes and their expression levels were higher in the A2 population than in the A1 population (*SI Appendix*, Fig. S3 *B* and *C*). *Col1a1* and *Col1a2*, which are the major scleral matrix genes, were down-regulated in the A2 population ($P = 0.015$ and 0.079, respectively) (*SI Appendix*, Fig. S3 *D* and *E*). In contrast, *Acta2*, a myofibroblast transdifferentiation marker, underwent up-regulation ($P = 0.026$) (*SI Appendix*, Fig. S3*F*). These results suggested that the A2 population (defined as "myofibroblast-like cells," Myofib-L) were myofibroblasts or an intermediate phenotype appearing during transdifferentiation of fibroblasts into myofibroblasts. Cells within the A1 population (defined as "fibroblast-like cells," Fib-L) represented quiescent fibroblasts.

Gene-Expression Profile Implicates eIF2-, mTOR-, and Hypoxia-Signaling Pathways in the Phenotypic Shift from A1 to A2 Cell Populations. Expression patterns for 660 genes underwent a significant change in the transition of Fib-L cells to Myofib-L cells [*t* tests with $P < 0.05$ and fold change of median transcripts per million (TPM) >2 or <0.5]. Pathway analysis showed that differentially expressed

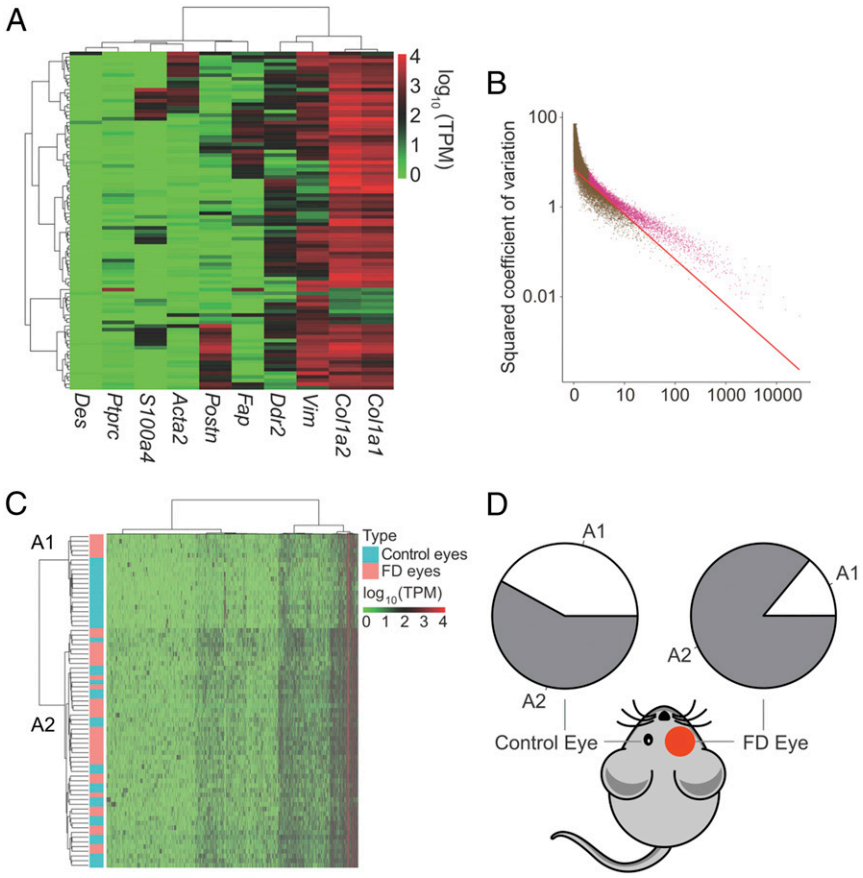

Fig. 1. Identification of two scleral fibroblast subpopulations by single-cell transcriptomic analysis. (*A*) Cell-type identification was based on log-transformed TPM values. Markers used for identifying cell types included collagen subtypes (*Col1a1* and *Col1a2*), a fibroblast marker (*Vim*), fibroblast transdifferentiation markers (*Ddr2*, *Fap*, *Postn*, *Acta2*, and *S100a4*), a leukocyte marker (*Ptprc*), and a myocyte marker (*Des*). (*B*) The expected CV^2 values of highly variable genes (pink dots) were less than the observed values. The red continuous curve represents the average expression levels. (*C*) Unsupervised hierarchical cluster analysis of 71 scleral fibroblasts based on the log-transformed TPM values of 4,463 genes with high CV^2 values. The *x* axis contains the genes with large CV^2 values, and the *y* axis indicates single scleral cells. Pink indicates FD eyes, and blue indicates control eyes. (*D*) Composition of A1 and A2 fibroblast subpopulations in FD and control eyes. The A2 subpopulation constituted 85.7% of the fibroblasts in the FD eyes vs. 58.3% in the control eyes ($P = 0.021$, χ^2 test).

genes (DEGs) were clearly enriched in 26 pathways (*SI Appendix*, Fig. S4), with nine pathways showing a significant predicted activity pattern (Fig. 2*A*). The top enriched pathways, i.e., eIF2 signaling, mTOR signaling, and hypoxia signaling in the cardiovascular system, mediate responses to hypoxic stress. Given a higher proportion of Myofib-L in FD eyes, this change indicated that these hypoxia-related signal pathways may be activated in FD eyes.

To validate the signaling pathways identified from scRNA-seq analysis in myopic scleras, we used RT-PCR to detect mRNA expression levels of eight DEGs from the top three pathways (*SI Appendix*, Table S4) in mice with 2 d of FD. In agreement with scRNA-seq analysis, scleral mRNA levels of these eight genes in the FD eyes were significantly increased compared with those in the control eyes (*SI Appendix*, Fig. S5*A*). Differential expression profiles of these genes after FD were specific to the sclera because expression in the retina remained unchanged (*SI Appendix*, Fig. S5*B*). Additionally, we compared the scRNA-seq data with that generated using bulk scleral tissue RNA sequencing (RNA-seq) to show similarities in expression features (*SI Appendix*, Fig. S6). The apparent consistency gave us more confidence in the scRNA-seq data. These data confirm that eIF2-, mTOR-, and hypoxia-signaling pathways in scleral fibroblasts are involved in myopia development.

To find the key modulators of the transition from Fib-L to Myofib-L, we divided the Myofib-L population into four subpopulations based on the results of hierarchical clustering (Fig. 2*B*). These four subpopulations were further ranked by expression cosine distance with the Fib-L population. This kind of ranking may indicate the process of the transition of Fib-L into Myofib-L in the sclera. Next, we employed Hypergeometric Optimization of Motif Enrichment software on 864 DEGs among the four subpopulations to identify candidate transcription factors mediating this transition. Thirty-six transcription factors were identified (*SI Appendix*, Table S5), including *Smad4* and *Hif1a*, which are effective transcription factors of the TGF-β–signaling pathway and the hypoxia-inducible factor-1α (HIF-1α) pathway, respectively. Seven transcription factors were expressed with a TPM >2 in at least one subpopulation, while only *Hif1a* was expressed over a dynamic range in association with the anticipated Fib-L–to–Myofib-L transition, with the highest level of expression occurring at the last stage (Fig. 2*C*). These results suggest that HIF-1α plays an important role in mediating the transition from fibroblasts to myofibroblasts.

The HIF-1α–Signaling Pathway Is Related to Genes Associated with Human Myopia. We next explored possible interactions between the top three significant signaling pathways and the development of myopia in humans. Using protein–protein interaction (PPI) networks, we investigated interactions of the risk genes of human myopia (*SI Appendix*, Table S6), determined in a previous genome-wide association study and linkage analysis (28, 29), with genes involved in these pathways. Of 145 myopia-risk genes, only nine had interactions with the eIF2-signaling pathway, and six had interactions with the mTOR pathway. On the other hand, nearly one-third of the myopia-risk genes interacted with genes involved in the HIF-1α–signaling pathway (45/145) (*SI Appendix*, Fig. S7). Of 27 pathologic myopia-risk genes, only three interacted with the eIF2-signaling pathway and one with the mTOR-signaling pathway. However, genes associated with pathologic myopia showed a borderline significance, with 10 of the 27 risk genes interacting with the HIF-1α–signaling pathway ($P = 0.07$, hyper-geometric distribution test) (Fig. 2*D*). Significant numbers of interactions were identified between genes in the HIF-1α pathway and the risk genes of myopia (mean interactions = 3.925, $P = 0.001$, bootstrapping) and pathologic myopia (mean interactions = 3.2, $P = 0.036$, bootstrapping).

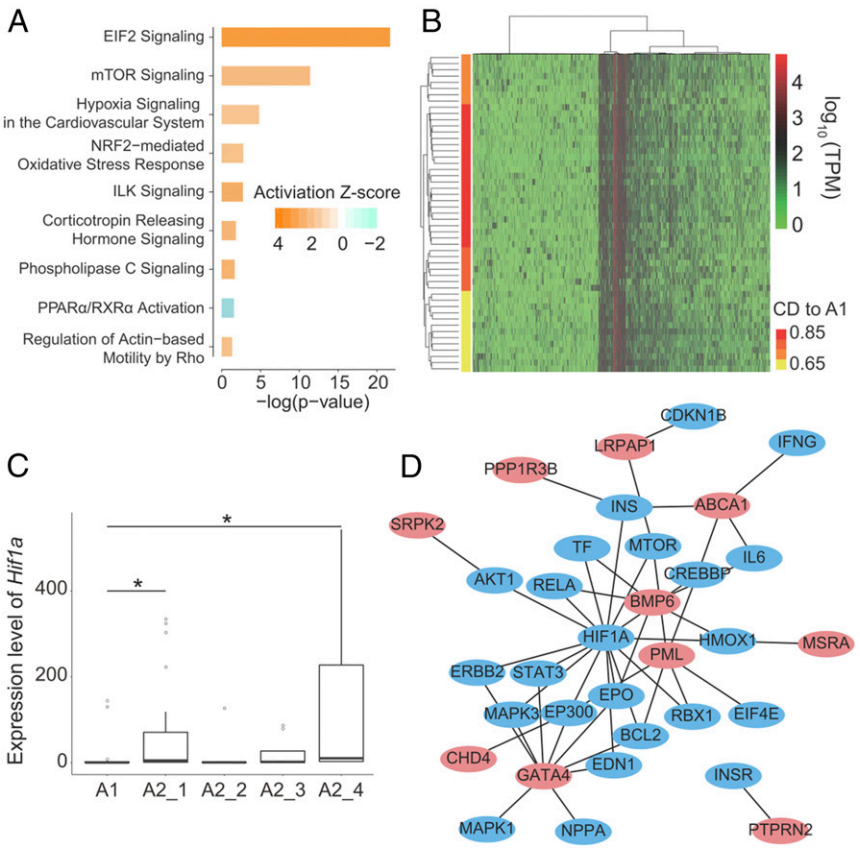

Fig. 2. Pathways and transcription factors underlying gene-expression changes during the transition of A1 to A2. (*A*) Pathways with enrichment $P <$ 0.01 and absolute activation Z-score >2 are shown. Almost all pathways were significantly activated in the A2 population except for PPAR/RXRα, which was inhibited. (*B*) Hierarchical cluster analysis of the A2 population. The *x* axis indicates the genes with large CV^2 values, and the *y* axis indicates the single scleral cells in the A2 population. The A2 population contained four subpopulations [the color gradient from yellow to red indicates the cosine distance (CD) to the A1 cell type, with those in yellow color being the closest to A1 cells and the red-colored ones being the farthest away]. Light to dark orange subpopulations represent intermediate cells. (*C*) Expression dynamics of *Hif1a* among different populations and subpopulations. The *x* axis is ranked by CD to A1, with the nearest subpopulation on the left (A2_1) and the farthest subpopulation on the right (A2_4). The A2_2 and A2_3 subpopulations are interspersed between them. Data are expressed as medians (interquartile ranges); $*P < 0.05$, Wilcoxon-rank test. (*D*) Relationship between human pathologic myopia-risk genes (red ovals) and genes in the HIF-1α–signaling pathway (blue ovals) according to the PPI network. The risk gene for pathologic myopia with the most interactions was *GATA4*, which is an important transcription activator involved in the developmental process. SNPs in this gene were reported to be associated with myopia in a French population (27).

Although myopia-risk genes exhibited no significant interactions with DEGs between the Fib-L and Myofib-L populations ($P = 0.68$, hyper-geometric distribution test), 27 pathologic myopia-risk genes had significant interactions with 40 of the 660 DEGs ($P = 0.00467$, hyper-geometric distribution test) (*SI Appendix*, Table S7). In addition, 6 of 141 human myopia risk genes (*PTPN5*, *NFIA*, *GNL2*, *KCNMA1*, *TBC1D23*, and *SPTAN1*) that have mouse homologs were found in DEGs between the Fib-L and Myofib-L ($P = 0.0409$, bootstrapping). However, none of the 27 human pathologic myopia-risk genes was observed in the DEGs. These findings emphasize that genes involved in the scleral cellular phenotypical changes in mouse model of myopia are strongly implicated in human myopia development.

Localized Scleral Hypoxia Is a Common Feature of Myopia. Given that hypoxia is a common factor among the risk genes of human pathologic myopia, we further determined the dynamic changes in HIF-1α protein, which is an indicator of tissue hypoxia (30), in mice with 2 d and 2 wk of FD. Scleral HIF-1α levels in the FD eyes were significantly increased compared with those in the control eyes after 2 d and 2 wk of FD (Fig. 3 *A* and *B*). No significant differences in retinal HIF-1α levels were detected between FD and control eyes at these two time points (Fig. 3 *C* and *D*). As expected, increased axial elongation was observed after 2 wk of FD (*SI Appendix*, Fig. S8). Such findings indicate the development of localized scleral hypoxia during myopia development.

Furthermore, we determined if scleral hypoxia is a common feature of myopia by measuring the changes in HIF-1α protein level in response to two different myopia-induction paradigms: FD and negative lens induction (LI) in guinea pigs. Both myopic stimuli significantly increased the scleral HIF-1α levels compared with those in the control eyes after 2 d and 1 wk of myopia induction and then declined to a level similar to that in the control eyes after 2 d of recovery (Fig. 4 *A*–*D*). Similar to mice, we did not detect significant changes in the retinal HIF-1α levels between the myopia-induced (FD or LI) eyes and their respective fellow controls at these time points (Fig. 4 *E*–*H*) despite the dynamic changes in eye growth at the above time points (*SI Appendix*, Fig. S9). These results strengthen our hypothesis that scleral hypoxia is a common feature of myopia.

Hypoxia Exposure-Induced Myofibroblast Transdifferentiation in Human Scleral Fibroblasts. To further explore the role of scleral hypoxic involvement in myopia, we used Western blots to examine myofibroblast transdifferentiation and collagen production in human scleral fibroblasts (HSFs) after reducing the levels of ambient oxygen to 5% O_2. In HSFs exposed to the hypoxic condition, there was increased expression of HIF-1α protein (Fig. 5*A*), the focal adhesion proteins vinculin (Fig. 5*B*) and paxillin (Fig. 5*C*), and the myofibroblast marker α-SMA (Fig. 5*D*). Simultaneously, there was a decrease in the expression of COL1A1 (Fig. 5*E*). Taken together, these results indicate that hypoxia may affect myopia development via scleral myofibroblast transdifferentiation.

Antihypoxia Drugs Inhibited the Progression of Experimental Myopia Without Affecting Normal Ocular Growth in Guinea Pigs. We further asked if amelioration of hypoxia affects myopia progression. The FD eyes of guinea pigs were given periocular injections of the antihypoxic drugs salidroside (31) or formononetin (32). After the injection of salidroside (10 μg per eye) or formononetin (5.0 μg per eye) for 4 wk, the scleral levels of HIF-1α, COL1α1, and α-SMA were determined by Western blot (Fig. 6 *A* and *B*). Injection of salidroside suppressed the up-regulation of HIF-1α (Fig. 6*A*). It also suppressed the down-regulation of COL1α1 in FD eyes (Fig. 6*A*). There were no changes in α-SMA levels in FD and control eyes in either the vehicle- or salidroside-injected group (Fig. 6*A*). Similarly, injection of formononetin suppressed the up-regulation of HIF-1α and the down-regulation of COL1α1 in FD

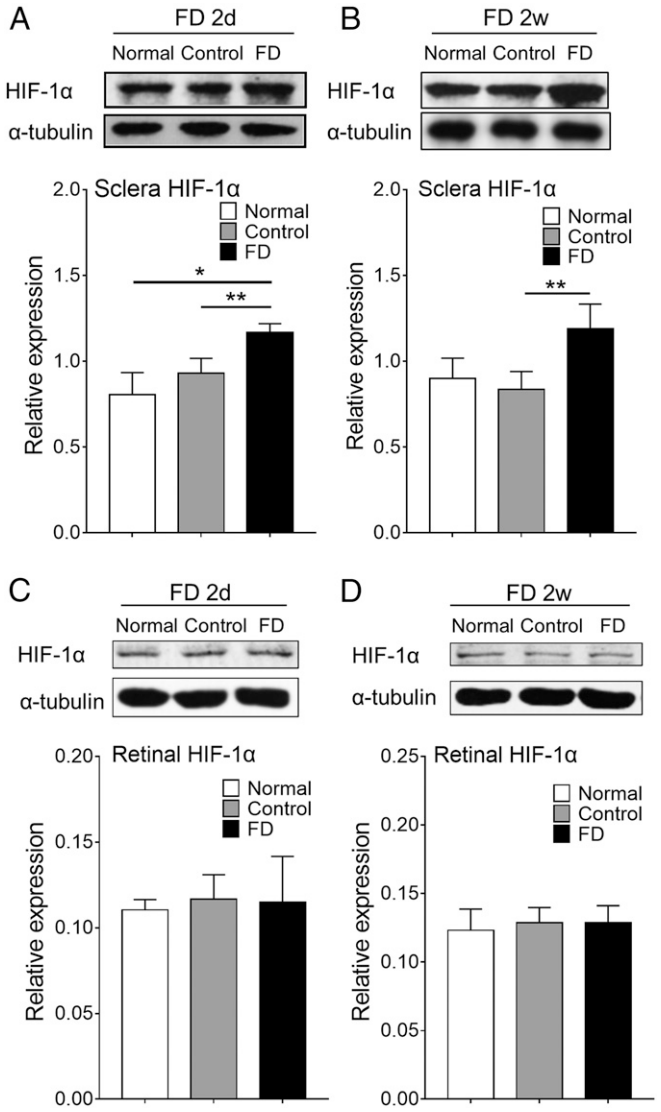

Fig. 3. Dynamic changes in the HIF-1α protein level during myopia development in mice. Western blot analysis of scleral (*A* and *B*) and retinal (*C* and *D*) HIF-1α expression in mice in response to FD for 2 d and 2 wk. Only right eyes from age-matched normal animals are shown. The bar graphs represent relative levels of HIF-1α from experiments (n = 3–6). Data are expressed as mean ± SEM. *$P < 0.05$; **$P < 0.01$; Student's t test.

eyes (Fig. 6*B*), while the α-SMA levels in FD and control eyes remained unchanged in both the vehicle- and the formononetin-injected group (Fig. 6*B*).

Importantly, daily injections of salidroside at the higher dose (10 μg per eye) for 4 wk significantly inhibited the development of myopia in FD guinea pigs compared with the lower dose (1 μg per eye) and vehicle injection (Fig. 6*C*). Elongation of axial length and vitreous chamber depth was also significantly inhibited with a higher dose of salidroside compared with the lower dosage and vehicle injection (Fig. 6 *D* and *E*). Daily injection with formononetin (0.5 μg per eye and 5.0 μg per eye) for 4 wk significantly inhibited myopia at both dosages (Fig. 6*F*). The elongation of axial length was also significantly inhibited at these dosages of formononetin (Fig. 6*G*), while the increase in the vitreous chamber depth showed a nonsignificant inhibition (Fig. 6*H*). In contrast, injecting normal guinea pigs with salidroside or formononetin did not induce any changes in refraction, axial length, or vitreous chamber depth (*SI Appendix*, Fig. S10). Collectively, these results indicate that scleral hypoxia plays critical roles during myopia development and that amelioration of hypoxia can suppress myopia progression through the down-regulation of HIF-1α and restoration of scleral collagen levels.

eIF2- and mTOR-Signaling Pathways Are Implicated in Myopia Development. Because eIF2 (33) and mTOR (34) signaling are associated with hypoxia, we further explored the effect of anti-hypoxic treatments on these two signaling pathways in myopic animal models. The phosphorylation levels of eIF2α and mTOR in sclera were determined after treatment as described above in guinea pigs (*SI Appendix*, Fig. S11 *A* and *B*). The ratio of phosphorylated eIF2α (P-eIF2α)/total eIF2α in the scleras of FD eyes after injection with the antihypoxic drugs salidroside (10 μg per eye) and formononetin (5.0 μg per eye) decreased significantly compared with that in the respective vehicle-control groups (*SI Appendix*, Fig. S11 *C* and *D*). The ratio of phosphorylated mTOR (P-mTOR)/total mTOR in the scleras of FD eyes after injection with salidroside was significantly decreased compared with the ratio in the vehicle-control groups (*SI Appendix*, Fig. S11*E*). Similarly, the ratio of P-mTOR/total mTOR in the scleras of FD eyes after injection with formononetin was significantly decreased compared with that in the control eyes (*SI Appendix*, Fig. S11*F*). This further highlights a possible interaction between hypoxia and the eIF2- and mTOR-signaling pathways during myopia development.

As the results from Ingenuity Pathway Analysis and antihypoxia treatment in FD guinea pigs showed the involvement of eIF2 and mTOR signaling in myopia, we further determined the role of these pathways in mediating the refractive development of mice. In FD mice, we administered i.p. injection of GSK2606414, an eIF2α phosphorylation inhibitor. After 2 wk of daily treatment (100 μg/kg or 330 μg/kg body weight), the interocular refractive difference between the FD and control eyes was significantly reduced in a dose-dependent manner (*SI Appendix*, Fig. S12*A*). In contrast, injection of either dose (200 μg/kg or 2,000 μg/kg) of everolimus, a mTOR inhibitor, had no significant effect on the interocular refractive difference (*SI Appendix*, Fig. S12*B*). In normal mice, the refractive change after injection with salubrinal (100 μg/kg or 330 μg/kg), an eIF2α dephosphorylation inhibitor, for the same duration was not significantly different from that in the vehicle group (*SI Appendix*, Fig. S12*C*). Normal mice injected with 200 μg/kg of MHY1485, an mTOR phosphorylation activator, progressed toward myopia compared with the vehicle group; however, a lower dose of MHY1485 (66 μg/kg) had no effect on refractive development (*SI Appendix*, Fig. S12*D*). In addition, Western blot analysis showed that daily i.p. injection of 330 μg/kg GSK2606414 or 200 μg/kg MHY1485 acts effectively on the scleral targets (*SI Appendix*, Fig. S12 *E* and *F*). Together, these results further support a role of hypoxia-related signaling pathways in myopia development.

Discussion

Various studies have shown that scleral ECM remodeling plays a critical role in myopia development (20); however, the triggering signal mechanisms involved in this process are currently unknown. Here, using the scRNA-seq methodology, we identified gene-expression changes associated with a phenotypic transdifferentiation of Fib-L toward Myofib-L during myopia development. Our data demonstrated that hypoxia is a key modulator for scleral ECM remodeling during myopia development. Two antihypoxic drugs, salidroside and formononetin, if delivered topically by eye drops, could have translational significance by suppressing myopia through their antihypoxic effects. Our results suggest that hypoxia is a target toward the treatment and management of this disease.

scRNA-Seq Reveals a Scleral Phenotypic Switch from Fib-L to Myofib-L via Activation of Hypoxic Signal During Myopia Development. Here we used single-cell analysis to resolve the mechanism of myofibroblast

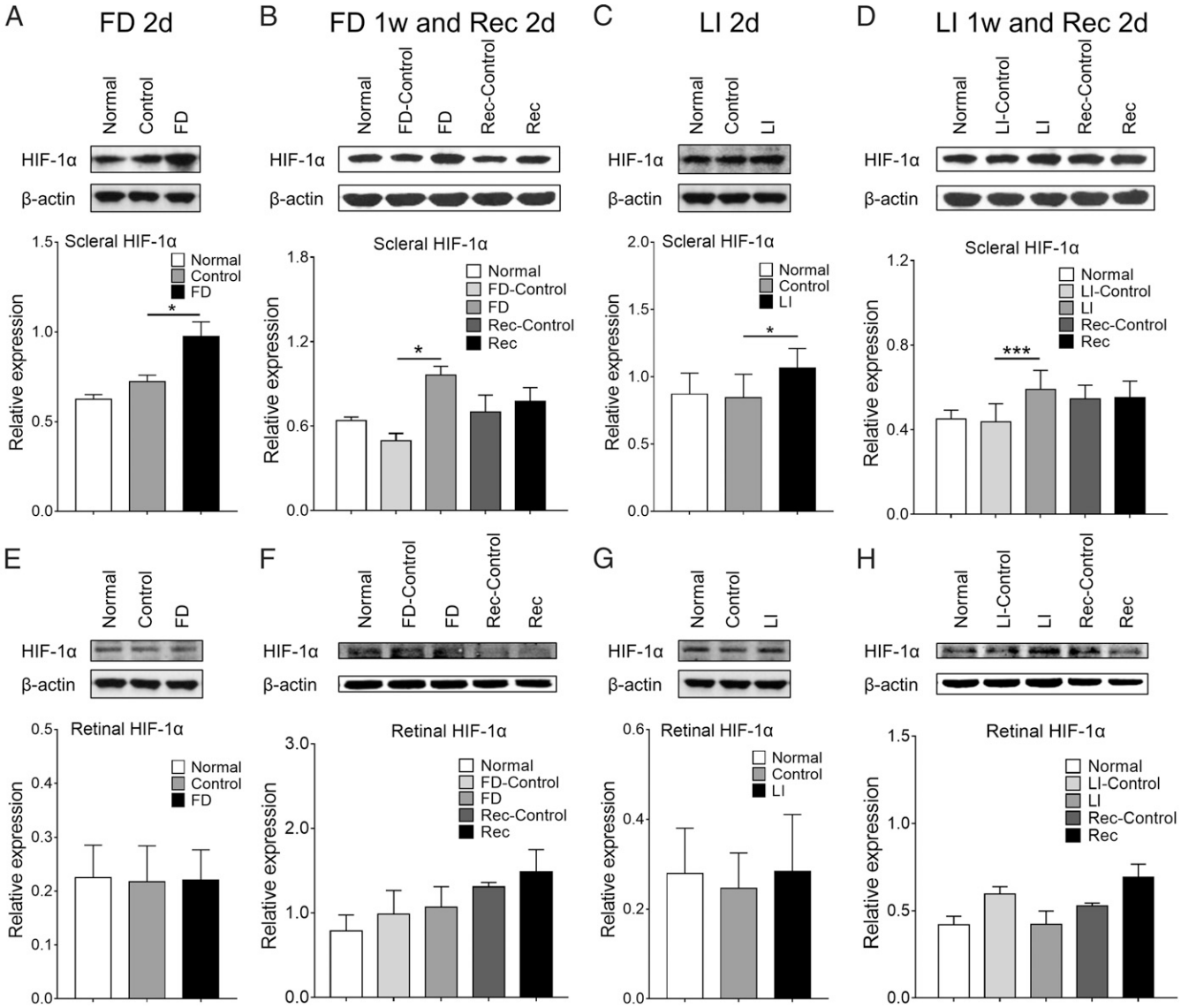

Fig. 4. Dynamic changes in HIF-1α protein level during myopia development in guinea pigs. (*A–D*) Western blot analysis of scleral HIF-1α expression in guinea pigs in response to FD (*A* and *B*) or LI (*C* and *D*) for 2 d or 1 wk and 2 d after recovery (Rec) from 1 wk of myopia induction. (*E–H*) Corresponding retinal HIF-1α expression levels in response to FD (*E* and *F*) or LI (*G* and *H*) at these time points. Only right eyes from age-matched normal animals are shown. Bar graphs represent HIF-1α levels from experiments (n = 3–4). Data are expressed as mean ± SEM. $^{*}P < 0.05$; $^{***}P < 0.001$; Student's t test.

transdifferentiation involved in myopia development. Traditional population-based genome-wide approaches are incapable of resolving this unsynchronized cellular phenotype shift process. In our current study, to obtain a sufficient number of cells for the scRNA-seq analysis, we separately pooled the FD scleral tissues and the control scleral tissues from six to eight animals to produce each suspension. This procedure could have limited the power of analysis. Despite this, we took advantage of the unique ability of the scRNA-seq technique to circumvent the cellular heterogeneity of sclera tissues. Thus, we identified two cellular populations with distinct gene-expression profiles and found a significant difference between them during myopia progression. Specifically, we found that the proportion of Myofib-L cells increased in sclera during myopia development, as evidenced by an increase in α-SMA expression. This is consistent with a previous report showing up-regulation of scleral α-SMA in myopic tree shrews (35). Scleral ECM remodeling occurs as a consequence of increases in myofibroblast transdifferentiation and is associated with the down-regulation of *Col1a1* and *Col1a2* gene expression, whereas degradative proteinases undergo up-regulation leading to increases in collagen turnover (20). These findings suggest an important role of the fibroblast-to-myofibroblast transdifferentiation during myopia development. This view is supported by an in vitro finding that imposed stress mediates myofibroblast transdifferentiation in fibroblast-populated collagen lattices that mimic the scleral microenvironment during myopia development (35). Also, an in vivo study showed that increasing the intraocular pressure for an extended period of time inhibited the ocular elongation in tree shrews, whose sclera is characterized by the presence of myofibroblasts (36). The transdifferentiated myofibroblast population in the sclera provides an offsetting contractile force that resists the persistent outward-directed force of intraocular pressure.

Notably, the myofibroblast phenotypic changes during myopia development are different from those occurring during wound healing (37). Unlike the transient type of myofibroblasts observed during wound healing, the myofibroblasts transdifferentiated during myopia development express lower levels of *Col1a1* and

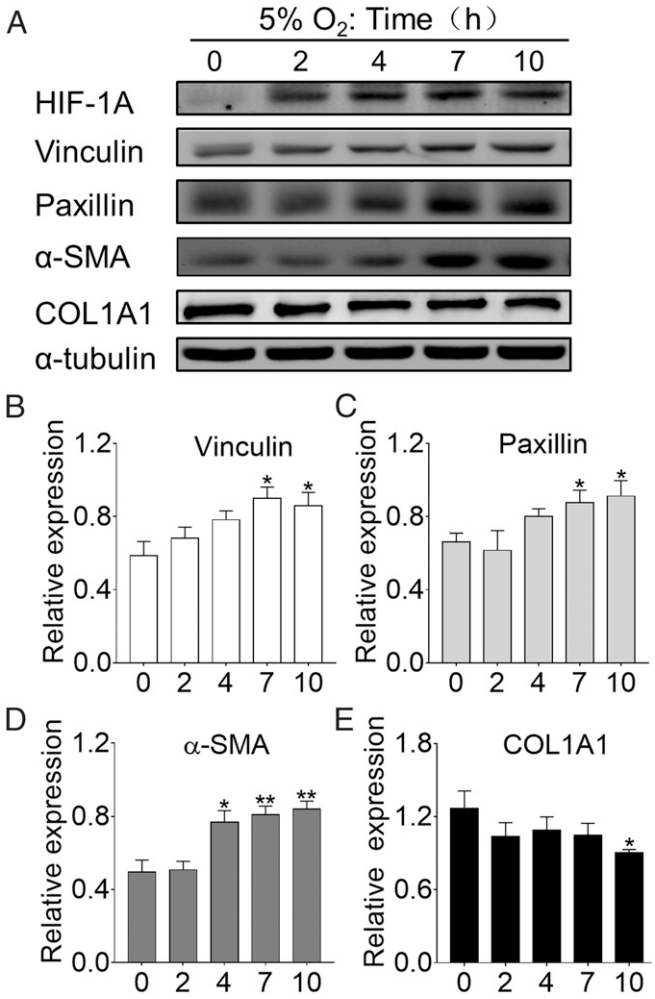

Fig. 5. Myofibroblast transdifferentiation in response to hypoxia in vitro. (*A*) HSFs exposed to 5% O_2 were analyzed by Western blot for the protein expression of HIF-1A, vinculin, paxillin, α-SMA, and COL1A1. (*B*–*E*) Bar graphs represent vinculin (*B*), paxillin (*C*), α-SMA (*D*), and COL1A1 (*E*) levels, respectively ($n = 4$). Data are expressed as mean ± SEM. $^*P < 0.05$; $^{**}P < 0.01$. Treatment duration: 2, 4, 7, or 10 h vs. control (0 h); Student's *t* test.

Col1a2. During wound healing, myofibroblasts exhibit a profibrotic phenotype with up-regulation of ECM components such as fibronectin and collagen. This phenotypic difference may be due to variations in the structural architecture of granulation tissues, i.e., wound healing is characterized by the formation of new capillaries containing vital nutrients (38), as opposed to the avascular scleral stroma. Thus, even though the scleral myofibroblasts acquire a contractile phenotype, the ability to mediate ECM remodeling is dependent on environmental cues (i.e., scleral hypoxia microenvironment).

Multiple lines of experimental evidence establish scleral hypoxia as a critical contributing factor in myopia development. First, scRNA-seq analysis revealed that myopia development is associated with the transdifferentiation of fibroblast to myofibroblast, whose major functional differences arise from activation of hypoxia-related pathways, including eIF2 signaling, mTOR signaling, and hypoxia signaling (Fig. 2*A*). Many genes that are involved in the HIF-1α–signaling pathway are associated with risk genes involved in human myopia or pathologic myopia (Fig. 2*D* and *SI Appendix*, Fig. S7). Second, while Guo et al. (39, 40) showed the possible involvement of scleral HIF-1α mRNA in myopia, our results showed that scleral HIF-1α protein levels increased in response to myopia induction in both mice and guinea pigs at 2 d (Figs. 3 and 4). Although we did not detect a change in HIF-1α levels in retina, we cannot exclude the possibility that the retina might undergo hypoxia-induced changes if the treatment persists longer. Third, in vitro exposure to hypoxia triggered the transdifferentiation of HSFs with increased expression of α-SMA, paxillin, and vinculin, along with reduced COL1A1 expression (Fig. 5), suggesting that the increase in scleral myofibroblast formation during myopia progression is associated with scleral hypoxia. Our results are consistent with previous studies that showed that hypoxia can enhance myofibroblast transdifferentiation in other tissues, such as skin (41), artery adventitia (42), and nasal polyps (43). Finally, antihypoxic treatments inhibited myopia development along with reduced levels of scleral HIF-1α (Fig. 6). Collectively, these findings suggest that the scleral microenvironment becomes hypoxic during myopia development, which triggers myofibroblast transdifferentiation, leading to reduced collagen biosynthesis.

The hypoxic signals may act as a common mediator for several signaling pathways during myopia. Our results showed that the elevated phosphorylation levels of eIF2α and mTOR were also suppressed by the antihypoxic drugs salidroside and formononetin in FD guinea pigs, suggesting the interaction between the hypoxic signal and the eIF2α and mTOR signal during myopia. Studies in renal tubular cells showed that hypoxia can enhance myofibroblast transdifferentiation through their interaction with TGF-β (44). As TGF-β is considered critical for myopia development (20), it may regulate scleral ECM remodeling through hypoxic signaling. Further experiments are needed to clarify the potential functional interactions of HIF-1α and TGF-β in scleral ECM remodeling.

Hypoxia May Be the Long-Sought Myopic Visual Signal Transduction Mechanism. Demonstration of scleral hypoxia during myopia development raises an important question: How can myopic visual signal transduction events mediate scleral hypoxia? Wallman and Winawer (12) speculated that visual signals are transduced in the retina and choroid and then are translated to produce mediators that affect myofibroblast transdifferentiation and ECM remodeling in the sclera. These changes then weaken the scleral framework, thereby accommodating increases in ocular elongation. The choroidal layer is uniquely positioned to translate and transfer myopic visual signals to the sclera, where they could affect ECM remodeling and ocular growth. However, the identity of the mediators acting between the choroid and sclera is unknown. Numerous studies have shown an association between myopia and choroidal thinning (45). In humans, myopic eyes with higher dioptric values have thinner choroids than those in fellow eyes with lower diopter values (46), and prolonged near work elicits an accommodation process that is associated with myopia development and choroidal thinning (47, 48). Choroidal thinning in humans with high myopia is also associated with reductions in both its stromal and vascular components (49). Further, changes in choroidal blood flow precede changes in choroidal thickness subsequent to a recovery period from FD in animal models (50). In addition, the increase of $\alpha\text{-SMA}^+$ cells in response to FD appeared mostly in the scleral layer close to choroid (51), suggesting the role of choroid in the transdifferentiation of scleral fibroblasts. Thus, altered choroidal vasculature and decreased choroidal blood flow may cause scleral hypoxia that triggers scleral myofibroblast transdifferentiation and altered scleral biomechanics.

Taking these findings together, we propose that myopia-related visual signals cause a decrease in choroidal capillary patency and blood flow, resulting in reduced levels of oxygen and nutrient supply to the neighboring avascular sclera (Fig. 7). Scleral hypoxia thus ensues, promoting myofibroblast transdifferentiation along with declines in collagen production through the accumulation of HIF-1α. These changes contribute

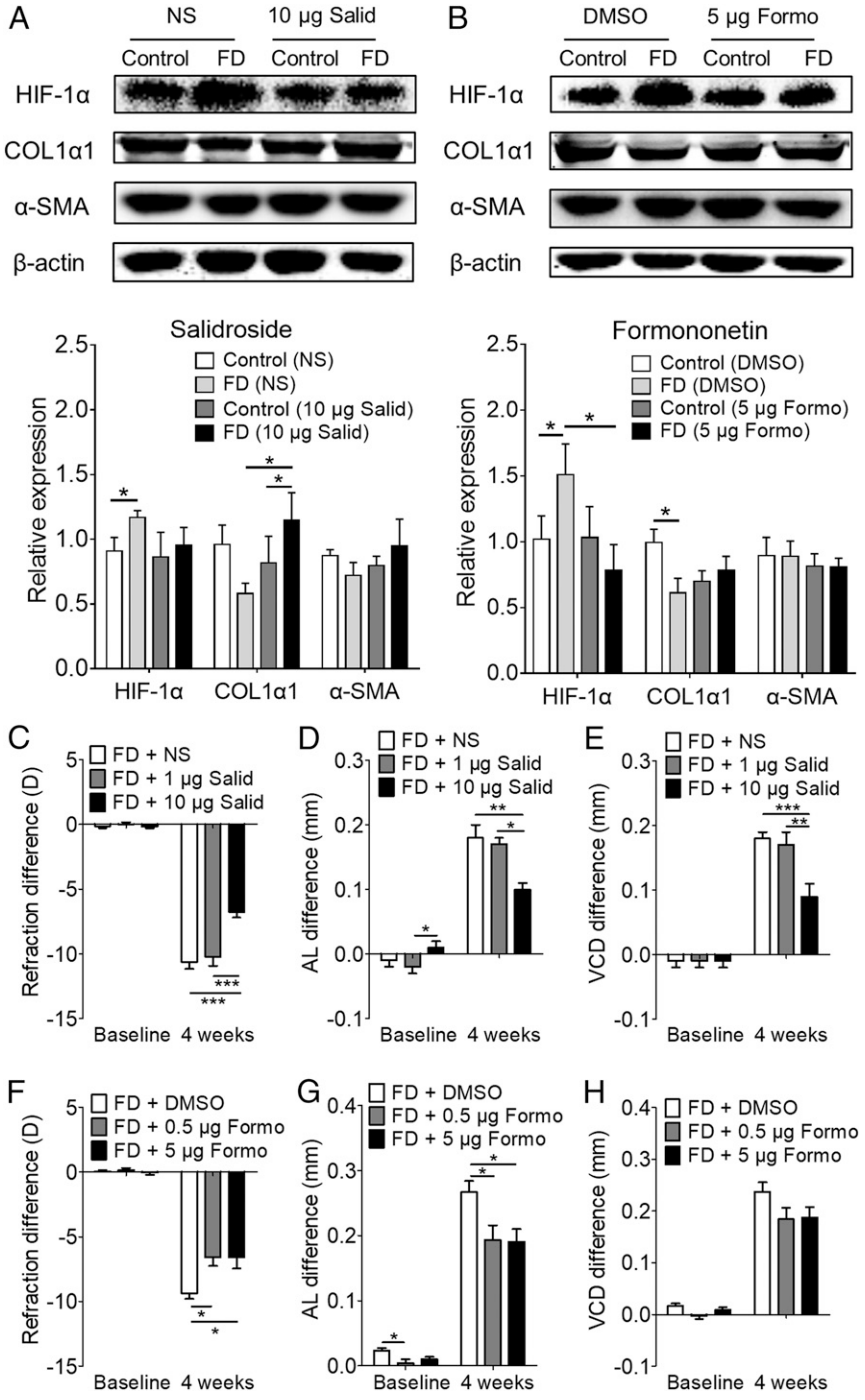

Fig. 6. Effect of antihypoxic drugs on myopia in guinea pigs with FD for 4 wk. (*A* and *B*) Protein levels of scleral HIF-1α, COL1α1, and α-SMA were detected by Western blot after periocular injection in FD eyes of salidroside(Salid) (10 μg per eye) (*A*) or formononetin (Formo) (5 μg per eye) (*B*) for 4 wk. Bar graphs represent HIF-1α, COL1α1, and α-SMA levels from experiments (n = 4–6). Data are expressed as mean ± SEM. $^*P < 0.05$; Student's t test. (*C*–*H*) Interocular differences (injected eye minus fellow untreated eye) in refraction (*C* and *F*), axial length (*D* and *G*), and vitreous chamber depth (*E* and *H*) in FD guinea pigs before and after 4 wk of treatment with normal saline (vehicle control, n = 13), salidroside,1 μg per eye (n = 10) or 10 μg per eye (n = 16) (*C*–*E*) or with 0.1% dimethyl sulfoxide (vehicle control, n = 18) or formononetin, 0.5 μg per eye (n = 19) or 5 μg per eye (n = 17) In *F*–*H*, data are expressed as mean ± SEM. $^*P < 0.05$; $^{**}P < 0.01$; $^{***}P < 0.001$; two-way repeated-measures ANOVA with Bonferroni multiple comparison. AL, axial length; D, diopter; DMSO, dimethyl sulfoxide; NS, normal saline; VCD, vitreous chamber depth.

to scleral thinning and weakening, ultimately resulting in excessive axial elongation. Further experiments are needed to clarify the detailed mechanisms between choroid and sclera.

Antihypoxic Treatment Offers Therapeutic Strategies for Myopia Control. Our study also demonstrated that antihypoxic treatments represent a therapeutic strategy for the control of myopia development. Salidroside and formononetin are active components of traditional Chinese medicines. Salidroside helps the body adapt to and resist stress (52) and has protective effects in vivo for hypoxia-induced cardiac apoptosis (53) and hypoxia-induced pulmonary hypertension (54). It antagonizes cobalt chloride-induced hypoxic effects in vitro (31, 55). Formononetin has a protective effect on hypoxia-induced retinal neovascularization (32) and, like salidroside, it also antagonizes cobalt chloride-induced hypoxic effects in vitro (56). We demonstrated that periocular injection of these two drugs suppressed myopia progression via antihypoxic effects as evidenced by a decrease in scleral HIF-1α accumulation. Notably, muscarinic receptor antagonists, such as atropine, that slow the clinical progression of myopia (57) also suppress myopia progression and choroidal thinning in chicks (58), suggesting that they might also act through amelioration of scleral hypoxia.

A noted feature of antihypoxic pharmacological strategy is the selective control of the pathological development of myopia without affecting normal ocular development. This is a critical

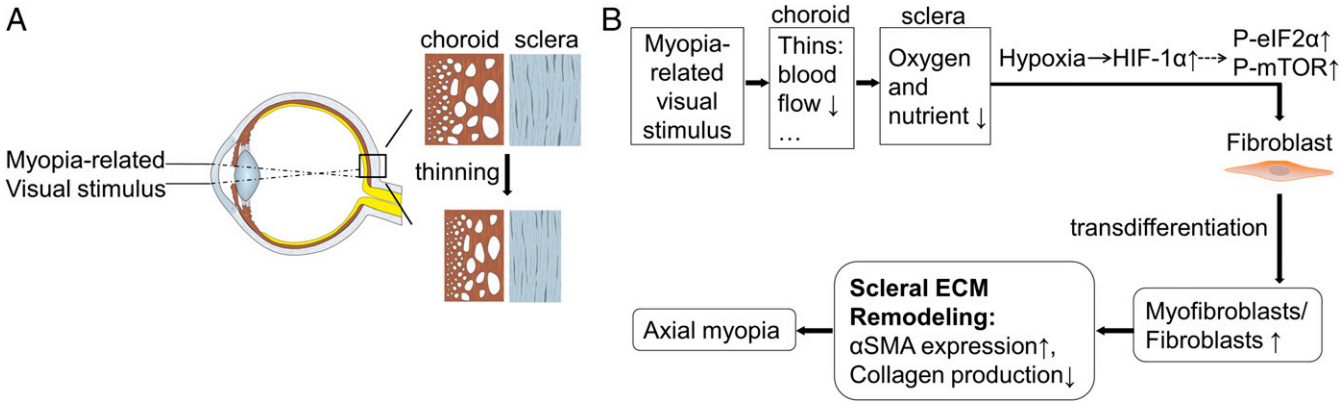

Fig. 7. Paradigm for myofibroblast transdifferentiation involved in the pathogenesis of myopia. (*A*) The choroidal layer thins rapidly followed by scleral thinning that results from ECM remodeling during myopic visual stimulus. (*B*) These myopia-related visual signals decrease choroidal blood flow that leads to an insufficient supply of oxygen and nutrients to the avascular sclera. Scleral fibroblasts first sense and quickly respond to the altered extracellular microenvironment through the accumulation of HIF-1α and enhanced phosphorylation levels of eIF2α and mTOR. This induces a phenotypic shift of fibroblast-like cells toward myofibroblast-like cells as well as a decrease in collagen production. As a result, the sclera becomes thinner and weaker. Consequently, axial length increases, and myopia ensues.

point, because myopia onset occurs at a young age that is critical for ocular development, and a drug that suppresses myopia must act mainly on targets specific to myopia pathogenesis rather than on normal ocular development. Our proposal to control myopia progression through management of scleral hypoxia is tenable by targeting the key transcription factor HIF-1α that is differentially regulated in a hypoxic condition and is rapidly degraded under the normoxic state. Indeed, our results showed an accumulation of scleral HIF-1α in myopic mice and guinea pigs, which is suggestive of the sclera being hypoxic during myopia. Importantly, antihypoxic drugs suppressed the progression of experimental myopia without affecting normal ocular growth in guinea pigs, demonstrating specificity toward myopia control. The suppression of myopia progression suggests the possible usefulness of these agents when delivered topically. Our findings suggest that this understanding of myopia pathogenesis mediated through choroid-regulated scleral hypoxia bears further exploration to determine the sources of the choroidal signals, the exact composition of the signals, and the scleral targets. This information may lead to clinical approaches in the management of myopia development and progression.

Materials and Methods

Detailed methodology is provided in *SI Appendix, SI Materials and Methods*.

Animal Experiments. The treatment and care of the animals was conducted according to the Association for Research in Vision and Ophthalmology statement for the use of animals in ophthalmic and vision research, and the protocol for handling animals was approved by the Animal Care and Ethics Committee at Wenzhou Medical University, Wenzhou, China (approval number: WYDW2014-0015).

Experimental myopia in mice (male C57BL/6 mice, about 3 wk old) was induced by monocular FD as previously reported (59). Two days after FD, the whole sclera of each eye was harvested separately for scRNA-seq analysis. To validate the changes in DEGs from scRNA-seq analysis, we used RT-PCR to examine eight genes (*SI Appendix*, Tables S4 and S8) in the scleras and retinas from mice after 2 d of FD and from age-matched normal mice. To validate the major finding relating to the role of hypoxia in myopia, we used Western blots to determine the dynamic changes in HIF-1α protein in retinas and scleras from mice after 2 d or 2 wk of FD. As it is unlikely that changes in refractive state and axial length will be apparent after a brief period of FD (2 d), and given that the mice may develop cataract or keratitis in response to anesthetic injections (ketamine) given twice in 2 d, we measured the refraction and ocular biometrics only at 2 wk after FD. These parameters were measured in independent sets of mice or guinea pigs so that the ocular tissues from those animals undergoing HIF-1α protein-expression assays were not affected by normal visual stimulus during ocular measurements before harvest.

In another set of experiments aimed at identifying the effects of the specific eIF2- and mTOR-signaling pathways on myopia development, FD mice were injected i.p. daily with GSK2606414, an eIF2α kinase PERK inhibitor, or everolimus, an mTOR inhibitor, for 2 wk. Age-matched normal mice were injected i.p. daily with salubrinal, an eIF2α dephosphorylation inhibitor, or MHY1485, a mTOR phosphorylation activator, for the same duration. Refraction was measured before and after 2 wk of injections. The effects of GSK2606414 and MHY1485 on the phosphorylation levels of eIF2α and mTOR, respectively, in the scleras were evaluated by Western blots in another set of FD and normal mice after two daily injections.

In addition, we used guinea pigs (*Cavia porcellus*, the English short hair stock, about 3 wk old) as a second in vivo model of induced myopia to validate the role of hypoxia signaling. Experimental myopia was induced via monocular FD or −4.00 diopter negative LI as previously reported (60, 61). The changes in HIF-1α protein expression were also examined in the scleras and retinas from guinea pigs exposed to FD or LI for 2 d or 1 wk and after 2 d of recovery from 1 wk of myopia induction. The refraction and ocular biometrics were repeatedly measured in an independent set of guinea pigs at the above time points. The larger eyes of guinea pigs enabled periocular injection of the antihypoxic drugs salidroside and formononetin in FD animals for 4 wk to determine if they ameliorated the induced myopia and altered the expression of hypoxia-related molecules. The effects of these drugs on normal ocular development were also determined in age-matched normal animals for 4 wk.

Experimental Hypoxia in Vitro in HSFs. To investigate the potential role of hypoxia on scleral ECM remodeling, HSFs were established and used as previously described (62). The cells were grown in DMEM supplemented with 10% FBS (Gibco) and 2 mM glutamine. All cells were grown at 37 °C in a 5% CO_2, humidified incubator. Cells were seeded at a density of 2.5×10^5 in 35-mm culture dishes for 24 h before hypoxic treatment. Growth medium was replaced when the cells reached 70–80% confluence; then the HSFs were exposed to the hypoxic protocol. The cells were placed in a three-gas incubator (Thermo Fisher Scientific) that maintained a low O_2 level of 5% for 2, 4, 7, or 10 h. Cells maintained under the normoxic condition (21% O_2) served as the control. At the end of the designated periods, the cells were lysed, and protein levels of HIF-1A, COL1A1, α-SMA, paxillin, and vinculin were determined by Western blot analysis.

Drug Preparation and in Vivo Injection, scRNA-Seq Procedure, RT-PCR, and Western Blot Analysis. Details of drug preparation and in vivo injection, the scRNA-seq procedure, RT-PCR, and Western blot analysis are provided in *SI Appendix, SI Materials and Methods*.

Statistical Analysis. Comparisons of two samples were performed using the two-tailed Student's *t* test or Wilcoxon rank test. Multiple comparisons were performed using one-way ANOVA and Bonferroni's multiple-comparisons

test. Comparisons of different treatments at different time points were done using two-way repeated-measures ANOVA with Bonferroni multiple-comparisons test. Comparisons of gene frequencies were performed using the χ^2 test. P values < 0.05 were considered statistically significant. Unless stated otherwise, continuous variables were presented as means ± SEM. Other descriptive statistics and tests used are indicated in the paper or in the figure legends and tables they support.

ACKNOWLEDGMENTS. The study was supported by National Natural Science Foundation of China Grants 81670886, 81422007, 81470659, 81170870, and 3147119; National Key Research and Development Program of China Grant 2016YFC20160905200; Natural Science Foundation of Zhejiang Province Grants LZ14H120001 and LQ16H120006; the Zhejiang Provincial Program for the Cultivation of High-Level Innovative Health Talents; the National Young Excellent Talents Support Program; and Chinese Academy of Sciences Strategic Priority Research Program (XDB13020500).

1. Wojciechowski R (2011) Nature and nurture: The complex genetics of myopia and refractive error. *Clin Genet* 79:301–320.
2. Dolgin E (2015) The myopia boom. *Nature* 519:276–278.
3. Holden BA, et al. (2016) Global prevalence of myopia and high myopia and temporal trends from 2000 through 2050. *Ophthalmology* 123:1036–1042.
4. Flitcroft DI (2012) The complex interactions of retinal, optical and environmental factors in myopia aetiology. *Prog Retin Eye Res* 31:622–660.
5. Leo SW; Scientific Bureau of World Society of Paediatric Ophthalmology and Strabismus (WSPOS) (2017) Current approaches to myopia control. *Curr Opin Ophthalmol* 28:267–275.
6. Wiesel TN, Raviola E (1977) Myopia and eye enlargement after neonatal lid fusion in monkeys. *Nature* 266:66–68.
7. Wallman J, Gottlieb MD, Rajaram V, Fugate-Wentzek LA (1987) Local retinal regions control local eye growth and myopia. *Science* 237:73–77.
8. Raviola E, Wiesel TN (1985) An animal model of myopia. *N Engl J Med* 312:1609–1615.
9. McBrien NA, Cornell LM, Gentle A (2001) Structural and ultrastructural changes to the sclera in a mammalian model of high myopia. *Invest Ophthalmol Vis Sci* 42:2179–2187.
10. Gottlieb MD, Joshi HB, Nickla DL (1990) Scleral changes in chicks with form-deprivation myopia. *Curr Eye Res* 9:1157–1165.
11. Avetisov ES, Savitskaya NF, Vinetskaya MI, Iomdina EN (1983) A study of biochemical and biomechanical qualities of normal and myopic eye sclera in humans of different age groups. *Metab Pediatr Syst Ophthalmol* 7:183–188.
12. Wallman J, Winawer J (2004) Homeostasis of eye growth and the question of myopia. *Neuron* 43:447–468.
13. Siegwart JT, Jr, Norton TT (2002) The time course of changes in mRNA levels in tree shrew sclera during induced myopia and recovery. *Invest Ophthalmol Vis Sci* 43:2067–2075.
14. Gentle A, Liu Y, Martin JE, Conti GL, McBrien NA (2003) Collagen gene expression and the altered accumulation of scleral collagen during the development of high myopia. *J Biol Chem* 278:16587–16594.
15. Mertz JR, Wallman J (2000) Choroidal retinoic acid synthesis: A possible mediator between refractive error and compensatory eye growth. *Exp Eye Res* 70:519–527.
16. McFadden SA, Howlett MH, Mertz JR (2004) Retinoic acid signals the direction of ocular elongation in the guinea pig eye. *Vision Res* 44:643–653.
17. Liu Q, Wu J, Wang X, Zeng J (2007) Changes in muscarinic acetylcholine receptor expression in form deprivation myopia in guinea pigs. *Mol Vis* 13:1234–1244.
18. McBrien NA, Jobling AI, Truong HT, Cottriall CL, Gentle A (2009) Expression of muscarinic receptor subtypes in tree shrew ocular tissues and their regulation during the development of myopia. *Mol Vis* 15:464–475.
19. Zhou X, Pardue MT, Iuvone PM, Qu J (2017) Dopamine signaling and myopia development: What are the key challenges. *Prog Retin Eye Res* 61:60–71.
20. McBrien NA (2013) Regulation of scleral metabolism in myopia and the role of transforming growth factor-beta. *Exp Eye Res* 114:128–140.
21. Zhou X, et al. (2010) Genetic deletion of the adenosine A2A receptor confers postnatal development of relative myopia in mice. *Invest Ophthalmol Vis Sci* 51:4362–4370.
22. Cui D, et al. (2010) Adenosine receptor protein changes in guinea pigs with form deprivation myopia. *Acta Ophthalmol* 88:759–765.
23. Watson PG, Young RD (2004) Scleral structure, organisation and disease. A review. *Exp Eye Res* 78:609–623.
24. Matthijs Blankesteijn W (2015) Has the search for a marker of activated fibroblasts finally come to an end? *J Mol Cell Cardiol* 88:120–123.
25. Hisatomi T, et al. (2007) Identification of resident and inflammatory bone marrow derived cells in the sclera by bone marrow and haematopoietic stem cell transplantation. *Br J Ophthalmol* 91:520–526.
26. Macosko EZ, et al. (2015) Highly parallel genome-wide expression profiling of individual cells using nanoliter droplets. *Cell* 161:1202–1214.
27. Meng W, et al. (2012) A genome-wide association study provides evidence for association of chromosome 8p23 (MYP10) and 10q21.1 (MYP15) with high myopia in the French population. *Invest Ophthalmol Vis Sci* 53:7983–7988.
28. Welter D, et al. (2014) The NHGRI GWAS Catalog, a curated resource of SNP-trait associations. *Nucleic Acids Res* 42:D1001–D1006.
29. Landrum MJ, et al. (2016) ClinVar: Public archive of interpretations of clinically relevant variants. *Nucleic Acids Res* 44:D862–D868.
30. Wang GL, Jiang BH, Rue EA, Semenza GL (1995) Hypoxia-inducible factor 1 is a basic-helix-loop-helix-PAS heterodimer regulated by cellular O2 tension. *Proc Natl Acad Sci USA* 92:5510–5514.
31. Xu ZW, et al. (2016) SILAC-based proteomic analysis reveals that salidroside antagonizes cobalt chloride-induced hypoxic effects by restoring the tricarboxylic acid cycle in cardiomyocytes. *J Proteomics* 130:211–220.
32. Wu J, et al. (2016) Formononetin, an active compound of *Astragalus membranaceus* (Fisch) Bunge, inhibits hypoxia-induced retinal neovascularization via the HIF-1α/VEGF signaling pathway. *Drug Des Devel Ther* 10:3071–3081.
33. Koumenis C, et al. (2002) Regulation of protein synthesis by hypoxia via activation of the endoplasmic reticulum kinase PERK and phosphorylation of the translation initiation factor eIF2alpha. *Mol Cell Biol* 22:7405–7416.
34. Humar R, Kiefer FN, Berns H, Resink TJ, Battegay EJ (2002) Hypoxia enhances vascular cell proliferation and angiogenesis in vitro via rapamycin (mTOR)-dependent signaling. *FASEB J* 16:771–780.
35. Jobling AI, Gentle A, Metlapally R, McGowan BJ, McBrien NA (2009) Regulation of scleral cell contraction by transforming growth factor-beta and stress: Competing roles in myopic eye growth. *J Biol Chem* 284:2072–2079.
36. Phillips JR, McBrien NA (2004) Pressure-induced changes in axial eye length of chick and tree shrew: Significance of myofibroblasts in the sclera. *Invest Ophthalmol Vis Sci* 45:758–763.
37. Gerarduzzi C, Di Battista JA (2017) Myofibroblast repair mechanisms post-inflammatory response: A fibrotic perspective. *Inflamm Res* 66:451–465.
38. Darby IA, Laverdet B, Bonté F, Desmoulière A (2014) Fibroblasts and myofibroblasts in wound healing. *Clin Cosmet Investig Dermatol* 7:301–311.
39. Guo L, Frost MR, He L, Siegwart JT, Jr, Norton TT (2013) Gene expression signatures in tree shrew sclera in response to three myopiagenic conditions. *Invest Ophthalmol Vis Sci* 54:6806–6819.
40. Guo L, Frost MR, Siegwart JT, Jr, Norton TT (2014) Scleral gene expression during recovery from myopia compared with expression during myopia development in tree shrew. *Mol Vis* 20:1643–1659.
41. Zhao B, et al. (2017) Hypoxia drives the transition of human dermal fibroblasts to a myofibroblast-like phenotype via the TGF-β1/Smad3 pathway. *Int J Mol Med* 39:153–159.
42. Short M, Nemenoff RA, Zawada WM, Stenmark KR, Das M (2004) Hypoxia induces differentiation of pulmonary artery adventitial fibroblasts into myofibroblasts. *Am J Physiol Cell Physiol* 286:C416–C425.
43. Moon YM, Kang HJ, Cho JS, Park IH, Lee HM (2012) Nox4 mediates hypoxia-stimulated myofibroblast differentiation in nasal polyp-derived fibroblasts. *Int Arch Allergy Immunol* 159:399–409.
44. Han WQ, et al. (2013) Hypoxia-inducible factor prolyl-hydroxylase-2 mediates transforming growth factor beta 1-induced epithelial-mesenchymal transition in renal tubular cells. *Biochim Biophys Acta* 1833:1454–1462.
45. Wang S, Wang Y, Gao X, Qian N, Zhuo Y (2015) Choroidal thickness and high myopia: A cross-sectional study and meta-analysis. *BMC Ophthalmol* 15:70.
46. Vincent SJ, Collins MJ, Read SA, Carney LG (2013) Retinal and choroidal thickness in myopic anisometropia. *Invest Ophthalmol Vis Sci* 54:2445–2456.
47. Ramamurthy D, Lin Chua SY, Saw SM (2015) A review of environmental risk factors for myopia during early life, childhood and adolescence. *Clin Exp Optom* 98:497–506.
48. Woodman-Pieterse EC, Read SA, Collins MJ, Alonso-Caneiro D (2015) Regional changes in choroidal thickness associated with accommodation. *Invest Ophthalmol Vis Sci* 56:6414–6422.
49. Gupta P, et al. (2017) Characterization of choroidal morphologic and vascular features in young men with high myopia using spectral-domain optical coherence tomography. *Am J Ophthalmol* 177:27–33.
50. Fitzgerald ME, Wildsoet CF, Reiner A (2002) Temporal relationship of choroidal blood flow and thickness changes during recovery from form deprivation myopia in chicks. *Exp Eye Res* 74:561–570.
51. Wu PC, et al. (2015) Chondrogenesis in scleral stem/progenitor cells and its association with form-deprived myopia in mice. *Mol Vis* 21:138–147.
52. Khanna K, Mishra KP, Ganju L, Singh SB (2017) Golden root: A wholesome treat of immunity. *Biomed Pharmacother* 87:496–502.
53. Lai MC, et al. (2014) Protective effect of salidroside on cardiac apoptosis in mice with chronic intermittent hypoxia. *Int J Cardiol* 174:565–573.
54. Huang X, et al. (2015) Salidroside attenuates chronic hypoxia-induced pulmonary hypertension via adenosine A2a receptor related mitochondria-dependent apoptosis pathway. *J Mol Cell Cardiol* 82:153–166.
55. Zhong X, Lin R, Li Z, Mao J, Chen L (2014) Effects of salidroside on cobalt chloride-induced hypoxia damage and mTOR signaling repression in PC12 cells. *Biol Pharm Bull* 37:1199–1206.
56. Sun M, et al. (2012) Formononetin protects neurons against hypoxia-induced cytotoxicity through upregulation of ADAM10 and sAβPPα. *J Alzheimers Dis* 28:795–808.
57. Grzybowski A, Armesto A, Szwajkowska M, Iribarren G, Iribarren R (2015) The role of atropine eye drops in myopia control. *Curr Pharm Des* 21:4718–4730.
58. Nickla DL, Zhu X, Wallman J (2013) Effects of muscarinic agents on chick choroids in intact eyes and eyecups: Evidence for a muscarinic mechanism in choroidal thinning. *Ophthalmic Physiol Opt* 33:245–256.
59. Schaeffel F, Burkhardt E, Howland HC, Williams RW (2004) Measurement of refractive state and deprivation myopia in two strains of mice. *Optom Vis Sci* 81:99–110.
60. Lu F, et al. (2006) Axial myopia induced by a monocularly-deprived facemask in guinea pigs: A non-invasive and effective model. *Exp Eye Res* 82:628–636.
61. Lu F, et al. (2009) Axial myopia induced by hyperopic defocus in guinea pigs: A detailed assessment on susceptibility and recovery. *Exp Eye Res* 89:101–108.
62. Qu J, et al. (2006) The presence of m1 to m5 receptors in human sclera: Evidence of the sclera as a potential site of action for muscarinic receptor antagonists. *Curr Eye Res* 31:587–597.